Physica Medica 127 (2024) 104837

Contents lists available at ScienceDirect

Physica Medica

journal homepage: www.elsevier.com/locate/ejmp

Influence of X-ray spectrum and bowtie filter characterisation on the accuracy of Monte Carlo simulated organ doses: Validation in a whole-body CT scanning mode

Gwenny Verfaillie [a,*], Jeff Rutten [a], Lore Dewulf [a], Yves D'Asseler [b,c], Klaus Bacher [a]

[a] Department of Human Structure and Repair, Ghent University, Proeftuinstraat 86 – Building N7, 9000 Ghent, Belgium
[b] Department of Nuclear Medicine, Ghent University Hospital, Corneel Heymanslaan 10, 9000 Ghent, Belgium
[c] Department of Diagnostic Sciences, Ghent University, Corneel Heymanslaan 10, 9000 Ghent, Belgium

ARTICLE INFO

Keywords:
Computed Tomography (CT)
Monte Carlo
Patient-specific dosimetry
Organ dose

ABSTRACT

Purpose: For patient-specific CT dosimetry, Monte Carlo dose simulations require an accurate description of the CT scanner. However, quantitative spectral information and information on the bowtie filter material and shape from the manufacturer is often not available. In this study, the influence of different X-ray spectra and bowtie filter characterisation methods on simulated CT organ doses is studied.
Methods: Using ImpactMC, organ doses of whole-body CTs were simulated in twenty adult whole-body voxel models, generated from PET/CT examinations previously conducted in these patients. Simulated CT organ doses based on the manufacturer X-ray spectra and bowtie filter data were compared with those obtained using alternative characterisation models, including spectrum generators and experimentally measured dose data. A total of four different X-ray spectra and one bowtie filter model were defined based on these data.
Results: For all X-ray spectra and bowtie filter combinations, estimated CT organ doses are within 6% from those resulting from simulations with the CT characterisation models provided by the manufacturer. While varying the bowtie filter model results in CT organ dose differences smaller than 1%, dose differences up to 6% are observed when X-ray spectra are not based on the quantitative data from the manufacturer.
Conclusions: Estimated organ doses slightly depend on the applied CT characterisation model. When manufacturer's data are not available, half-value layer and dose measurements provide sufficient input to obtain equivalent X-ray spectra and bowtie filter profiles, respectively.

1. Introduction

Over the past decades, the use of computed tomography (CT) has increased significantly. Due to new techniques, protocols and technologies its application exceeded beyond diagnostic imaging towards screening for lung and colon cancer, and minimally invasive procedures. In addition, the use of CT in hybrid nuclear medicine imaging (PET/CT and SPECT/CT) is growing as well. This widespread use for different clinical purposes together with the growing concern about the long-term effects of radiation exposure, especially the risk of cancer, leads to the need for accurate dose estimations [1,2].

Using the effective or water-equivalent diameter metric, introduced by the AAPM Task Groups 204 and 220 [3,4], the CT dose indicator volume CT dose index ($CTDI_{vol}$) can be scaled to incorporate the size of the patient resulting in a size-specific dose estimate (SSDE). Nevertheless, accurate individual organ dose estimations to assess potential radiation risks are needed. For this purpose, easy-to-use dose calculation tools such as CT-Expo [5], WAZA-ARI [6], VirtualDose [7] and NCICT [8] were developed. However, they are often limited in the number of available phantoms or lack accurate implementation of automatic tube current modulation. CT-Expo, for instance, only employs mathematical phantoms, including the adult Adam and Eva phantom, a child and a baby phantom. Although WAZA-ARI already uses voxel phantoms to estimate organ doses, the adult male and female phantoms only represent the average Japanese body type [9]. In addition, there are only four adult and five paediatric phantoms available for each gender.

* Corresponding author.
E-mail addresses: gwenny.verfaillie@ugent.be (G. Verfaillie), jeff.rutten@ugent.be (J. Rutten), lore-dewulf@hotmail.com (L. Dewulf), yves.dasseler@ugent.be (Y. D'Asseler), klaus.bacher@ugent.be (K. Bacher).

https://doi.org/10.1016/j.ejmp.2024.104837
Received 8 February 2024; Received in revised form 5 September 2024; Accepted 18 October 2024
Available online 25 October 2024

VirtualDose, on the other hand, includes 25 virtual patients in total. These include a set of male and female adult voxel phantoms of various heights and weights, paediatric male and female phantoms at five ages, the RPI adult male and female phantom and pregnant females at three gestational stages. Meanwhile, NCICT incorporates a library of 351 paediatric and adult male and female voxel phantoms of various heights and weights (paediatric: 85 male and 73 female; adult: 100 male and 93 female), the ICRP reference paediatric and adult phantoms, and eight pregnant phantoms containing detailed foetus models at various gestations. Automatic tube current modulation can be activated in all four tools. However, its implementation can be different. In CT-Expo it is only available for adults while it has only recently been made accessible in NCICT. Nevertheless, organ sizes and positions differ from patient to patient making it, even with a large library of voxel phantoms, impossible to estimate patient-specific organ doses. Therefore, dedicated Monte Carlo (MC) frameworks using patient-specific voxel geometries were established. These individualised 3D voxel models can be created based on clinically available CT data of the patient.

Monte Carlo frameworks allow, next to the implementation of patient-specific anatomical models, an accurate description of the X-ray modality. For CT examinations, characterisation of the CT scanner includes describing the geometrical, spectral and shaped filter characteristics. The necessary geometrical information can easily be found in the technical reference manual of the system. However, to model the X-ray spectrum and bowtie filter the situation is different. Ideally, quantitative data is provided by the manufacturer. This means the number of photons at each energy level for the X-ray spectrum, while for the bowtie filter the varying thicknesses with increasing fan angle position are described for each material out of which the bowtie filter is made up. Based on non-disclosure agreements, some manufacturers also provide this quantitative X-ray spectrum and bowtie filter information. Nevertheless, in most cases, these data are not available. Fortunately, other methodologies exist to determine X-ray spectra and model shaped filters. Research of for example Tucker et al. [10] and Poludniowski et al. [11] resulted into generators to create an artificial X-ray spectrum based on information about the tube potential, anode angle and amount of filtration. The latter may be specified by the manufacturer separately for all inherent tube filtration present after signing a non-disclosure agreement. On the other hand, Turner et al. [12] presented an *equivalent* source model to describe the energy spectrum and filtration based on half-value layer and bowtie filter profile measurements, respectively, without the need of manufacturer's data. Meanwhile Boone [13] and McKenney et al. [14] developed the COBRA method to compute the angle-dependent bowtie filter attenuation and thickness while Kramer et al. [15] created a mathematical bowtie model.

Although newly developed methodologies to characterise the X-ray spectrum or bowtie filter of a CT scanner are evaluated by comparing the accuracy of CTDI simulations with measured CTDI values, their results are almost never compared with those obtained when quantitative manufacturer's data is used instead. In addition, when simulation results were compared, this was done using the IEC CT dosimetry phantoms [12] or, in a rare case, using an anthropomorphic phantom [15]. Therefore, the purpose of this study was to estimate the influence of various X-ray spectrum and bowtie filter modelling techniques, including those based on the use of quantitative manufacturer's data, on Monte Carlo simulated CT organ doses. By using voxel models created based on clinical whole-body (WB) CT images, the accuracy of *patient-specific CT organ doses* obtained through Monte Carlo simulations performed with X-ray spectrum and bowtie filter models that differ from the quantitative models from the manufacturer was studied.

2. Materials and methods

2.1. Patients and voxel models

Whole-body CT images of twenty adult patients, acquired during a whole-body PET/CT examination on a 40-slice Siemens Biograph mCT Flow (Siemens Healthineers, Germany), were collected retrospectively from the institutional Picture Archiving and Communication System (PACS). The ten male and female patients were chosen in such a way as to assure a wide variety in Body Mass Index (BMI) (Table 1). To be suitable for accurate dose estimations, the reconstructed Field of View (FOV) of the CT scans included the entire cross-section of the patient. All CT data was anonymised according to the hospitals anonymization policy to comply with the current General Data Protection Regulation (GDPR) rules. Patient-related information, represented by unique identifiers (tags), in the DICOM header of the images was thus completely removed or replaced by de-identified information. Only data concerning patient sex, age, length and weight was kept. The retrospective use of the CT images was approved by the institutional ethical committee.

Based on the data of the 512 x 512 DICOM images, a patient-specific 3D whole-body voxel model was created for each patient with 0.9727 x 0.9727 x 3 mm^3 voxel size.

2.2. Monte Carlo dose simulations

To estimate patient-specific CT organ doses, Monte Carlo (MC) simulations were performed with ImpactMC 1.6 (CT Imaging GmbH, Erlangen Germany). This patient-specific dose calculation tool combines Monte Carlo algorithms with scanner specific parameters such as geometric, spectral and shaped filter characteristics, and patient-specific voxel models based on patient CT images. In this way, the software calculates individualised 3D dose distributions, considering all relevant photon interaction processes [16,17]. To calibrate the simulation software, the air kerma free-in-air in the isocenter of the CT was measured using a pencil beam ionisation chamber (Model 10X6-3CT, Radcal Corporation, USA). The Monte Carlo software ImpactMC was validated by several research groups. Schmidt et al. [18], Deak et al. [17], Myronakis et al. [19] and Chen et al. [16] all validated the software based on the comparison of simulated and measured CTDI values using either the IEC CT body and/or head dosimetry phantom. While Schmidt et al. [18] also compared their results with those obtained from Monte Carlo programs based on the EGS4 platform and published values, Deak et al. [17] and Myronakis et al. [19] also performed validation measurements using anthropomorphic phantoms of various sizes.

In this study, whole-body CT examinations, from head to mid-thigh, were simulated using the scan parameters of a diagnostic whole-body CT on a Siemens Biograph mCT Flow. Helical scans were simulated at 120 kV with a rotation time of 0.5 s, a beam collimation of 19.2 mm and a pitch of 0.7 (Table 2). To integrate tube current modulation (TCM), the tube current value from the DICOM header of each reconstructed image was extracted using an in-house developed Fiji/ImageJ macro. Because of the TCM system available on the simulated CT scanner (CARE Dose4D), each tube current value is the average of the angularly and longitudinally modulated values applied over the gantry rotation used to reconstruct this image [20–25]. To ensure the speed and accuracy of the Monte Carlo simulation, the number of interacting photons was chosen to be 10^{10} for all simulations. In order to convert the CT values of the input whole-body patient CT images into density values the standard conversion curve incorporated in the ImpactMC software was used [26]. The assumed relationship is shown in Fig. 1.

Table 1
Summary of mean (minimum – maximum) age, length, weight and BMI of the study population.

Study population	Age (years)	Length (m)	Weight (kg)	BMI (kg/m^2)
10 females	64 (25 – 86)	1.63 (1.50 – 1.70)	63 (40 – 87)	24 (16 – 34)
10 males	65 (45 – 79)	1.77 (1.62 – 1.93)	75 (51 – 105)	24 (16 – 33)

Table 2
Summary of exposure parameters for a diagnostic whole-body CT at a Siemens Biograph mCT Flow PET/CT.

Parameter	Siemens whole-body CT
Tube voltage (kV)	120
Tube current (mA)	ATCM*
Rotation time (s)	0.5
Pitch	0.7
Beam collimation (mm)	19.2
Scan FOV (mm)	500
Scan start	head
Scan end	mid-thigh

* Automatic Tube Current Modulation

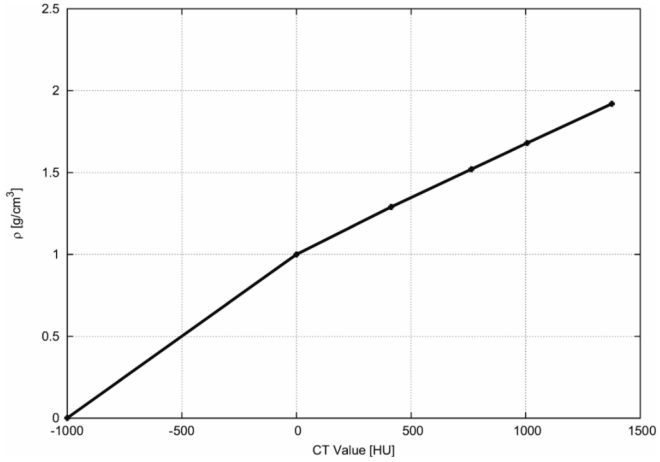

Fig. 1. Standard conversion from CT values in Hounsfield Units (HU) to density values in g/cm^3 as performed by the ImpactMC software (from the ImpactMC user guide [26]).

2.3. CT scanner characterisation

For scanner-specific Monte Carlo (MC) dose computations, information on the geometric, spectral and shaped filter characteristics of the CT scanner are needed as input parameters. This section describes how these characteristics were determined to model the CT part of a Siemens Biograph mCT Flow PET/CT.

2.3.1. Geometric specifications

The geometrical specifications, such as the focus to isocenter distance (595 mm) and fan angle (0.7955 rad), were derived from the specific data elements, DICOM tags, in the DICOM header of the CT images. However, they could be extracted from the technical reference manual of the system as well.

2.3.2. X-ray spectrum determination

An important input parameter for Monte Carlo dose simulations is the spectrum of the X-ray beam, which is determined by its tube potential and the first half-value layer (HVL). The ImpactMC software expects a text file wherein the spectrum is specified as the number of photons at each energy level [26]. If necessary, the number of photons, binned in 1 keV steps, will be normalised by the software. However, to specify the X-ray beam spectrum different possibilities exist. Which method can be used depends on the data made available by the manufacturer. This has an impact on the accuracy of simulated CT organ doses. Therefore, in this study, five X-ray beam spectra models were generated using different methodologies for the tube voltage of 120 kV, which is the standard tube voltage for diagnostic whole-body CT scans at the Siemens Biograph mCT Flow PET/CT as described before. A schematic overview of these five models and the data that was used to obtain them is shown in Fig. 2. Subsequent paragraphs explain this in more detail.

2.3.2.1. Quantitative spectral information from the manufacturer. The first X-ray model was based on the quantitative spectral information for 120 kV provided by the manufacturer which was specified as the number of photons at each energy level (Fig. 2 – X-ray spectrum model (1)). Because normalisation of the number of photons is done by the Monte Carlo software, if necessary, the *provided spectral information* could be directly used as input for the dose simulations. A graphical visualisation of the spectrum is shown in Fig. 3.

2.3.2.2. Spectrum generators. Secondly, two artificial X-ray spectra were created using so called spectrum generators. For the first model the *ImpactMC integrated spectrum generator* (based on work of Tucker et al. [10]) was used, while for the second spectrum *SpekCalc* (based on work of Poludniowski et al. [11]) was applied. In both tools, the user needs to select the tube potential, the anode angle and the amount of filtration in mm (Fig. 2 – X-ray spectrum model (4) and (5)). The latter can be defined for different materials separately. In this study, 120 kV was selected as tube potential. Information on the anode angle and amount of filtration (all materials and their corresponding thicknesses) of the X-ray tube was provided by the manufacturer. The resulting spectrum models are visualised in Fig. 3. Due to a non-disclosure agreement we cannot disclose the specific details about the anode angle and amount of filtration. However, some of this information can be found in the technical specifications of the CT scanner. Nevertheless, the inherent tube filtration will often be described in equivalent aluminium thickness instead of the thickness of each separate filter material.

2.3.2.3. Half-value layer measurements. Finally, the methodology as described by Turner et al. [12] for equivalent energy spectra in CT was used. Because it only requires physical measurements and calculations no information from the manufacturer is needed. First, the half-value layer of the 120 kV spectrum was experimentally derived. To do this, a calibrated pencil beam ionisation chamber (Model 10X6-3CT, Radcal Corporation, USA) was placed free-in-air at the isocenter of the CT. Thin aluminium slabs with a thickness of 2, 1 and 0.5 mm were then stepwise added to the beam path, until the measured air kerma was less than half the initial air kerma measured without extra aluminium. In this way, the half-value layer was determined as the amount of aluminium needed to halve the initial air kerma. The measurements were carried out at a fixed tube current–time product. To keep the X-ray tube stationary, measurements were performed in the 2D projection mode. Because CT couch movement is inevitable in this scan mode, the ionisation chamber was placed in the isocenter of the CT using a tripod positioned at the bottom of the gantry. In this study, table movement in the field of view could be avoided. As a result the X-ray tube was positioned at the bottom and the aluminium slabs could simply be placed on the gantry. However, if this is not possible, measurements can also be performed in lateral 2D projection mode. The experimental set-up is illustrated in Fig. 4.

Secondly, an equivalent spectrum was generated with an in-house developed MATLAB code (Mathworks, USA) with added SPEKTR tool [27]. The code started from a soft spectrum and iteratively added layers of aluminium until the difference between the simulated and measured half-value layer was minimal. The resulting spectrum was binned in 1 keV steps to be used in a Monte Carlo simulation. A flowchart of this iterative process is shown in Fig. 5.

Next to the tube potential and the amount of added filtration, the SPEKTR tool also expects the ripple factor (percentage voltage ripple) as input parameter for the generation of equivalent energy spectra. Turner et al. [12] used a 25% voltage ripple, while the study of Yang et al. [28] started with a ripple factor of 0%. In this study, *equivalent energy spectra* for CT were created applying a voltage ripple of both *0%* and *25%* (Fig. 2

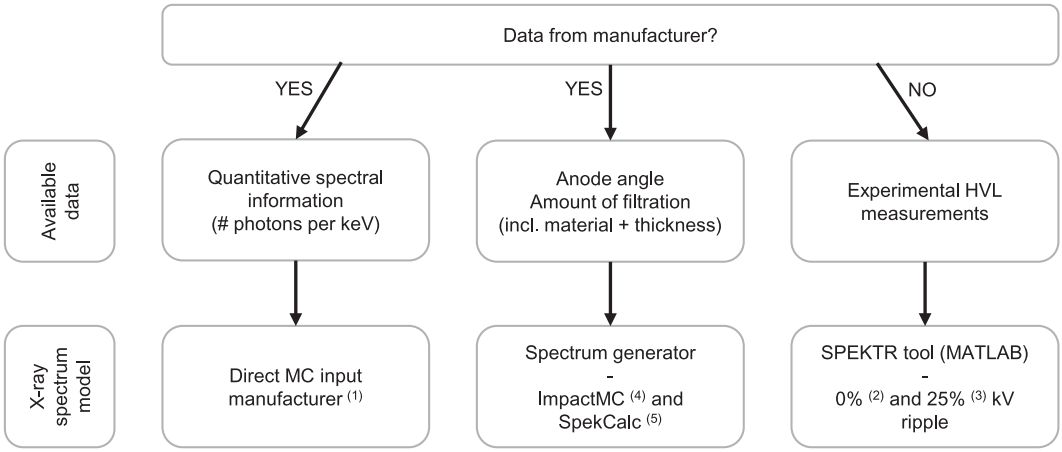

Fig. 2. Schematic overview of the five created X-ray beam spectrum models: (1) – X-ray spectrum model as provided quantitatively by the manufacturer; (2) and (3) – equivalent energy spectrum based on half-value layer measurements and created with the SPEKTR tool applying a 0% and 25% voltage ripple, respectively; (4) and (5) – X-ray spectrum model generated using the ImpactMC integrated spectrum generator and SpekCalc, respectively, based on the anode angle and filtration data provided by the manufacturer.

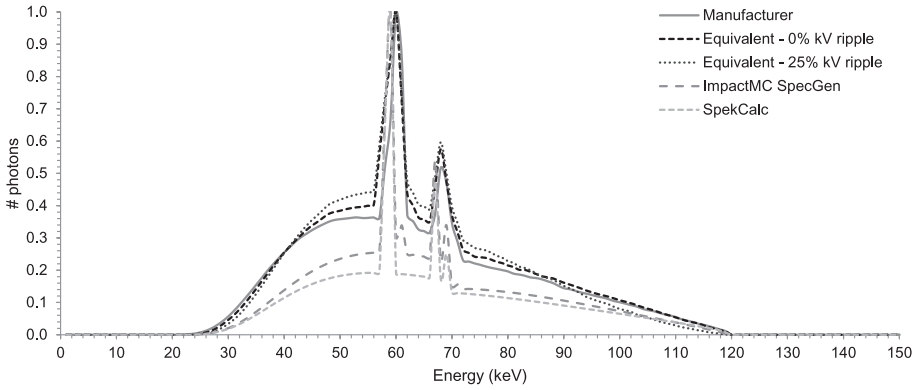

Fig. 3. Graphical overview of the X-ray spectrum models for a tube voltage of 120 kV. The X-ray spectra models were, respectively, provided quantitatively by the manufacturer, created using the SPEKTR tool applying a 0 % or 25 % voltage ripple after half-value layer measurements, and generated with the ImpactMC integrated spectrum generator or SpekCalc based on the anode angle and filtration data provided by the manufacturer.

– X-ray spectrum model (2) and (3)). These two resulting X-ray spectrum models are given in Fig. 3 together with the other three models.

2.3.3. Shaped bowtie filter model

To characterise the shaped filter, two bowtie filter models were created. The first model was based on data provided by the manufacturer, which defined the attenuation of the bowtie (w.r.t. the detector signal) as a function of the fan angle. This information was converted to an input file suitable for the Monte Carlo software.

The second model characterised the bowtie filter based on dose measurements performed free-in-air. For this purpose, a calibrated pencil beam ionisation chamber (Model 10X6-3CT, Radcal Corporation, USA) was used. Dose measurements were incrementally obtained by moving the ionisation chamber in 1 cm intervals from the isocenter while keeping the X-ray tube stationary (Fig. 6). Since the bowtie filter is symmetric, only one side of the bowtie filter needed to be defined together with the focus to isocenter distance and the increment distance between the measurement points. However, due to uncertainties in positioning, dose measurements were performed in both the +x and −x direction. The dose at each increment position was then calculated as the mean of the measured dose values in both directions at the same distance from the isocenter.

2.3.4. Impact of CT scanner characterisation model on estimated organ doses

To evaluate the effect of the X-ray spectrum and bowtie filter characterisation model on estimated CT organ doses, each of the previously determined models was used in the Monte Carlo simulations. Because five X-ray spectrum and two bowtie filter models were defined, this means that ten Monte Carlo dose simulations were performed for each of the twenty patients included in this study. An overview of these different scenarios is given in Table 3.

2.4. Organ dose calculation

2.4.1. Delineation of organs

To delineate the radiosensitive organs and tissues of interest, the open source software tools Fiji/ImageJ [29,30] and 3D Slicer [31] were used. For the lungs, bones (ribs/spine) and liver, the regions of interest (ROIs) were obtained semi-automatically. The breast (female patients), heart, kidneys, thyroid and oesophagus on the other hand were delineated manually. This was done by a medical physicist.

2.4.2. Patient-specific organ doses

A Monte Carlo dose calculation with ImpactMC results in a 3D dose distribution based on the physical properties (i.e. attenuation, composition and size) of the input patient CT scan. Overlaying the contours of each organ on the corresponding slices of the dose distribution results in

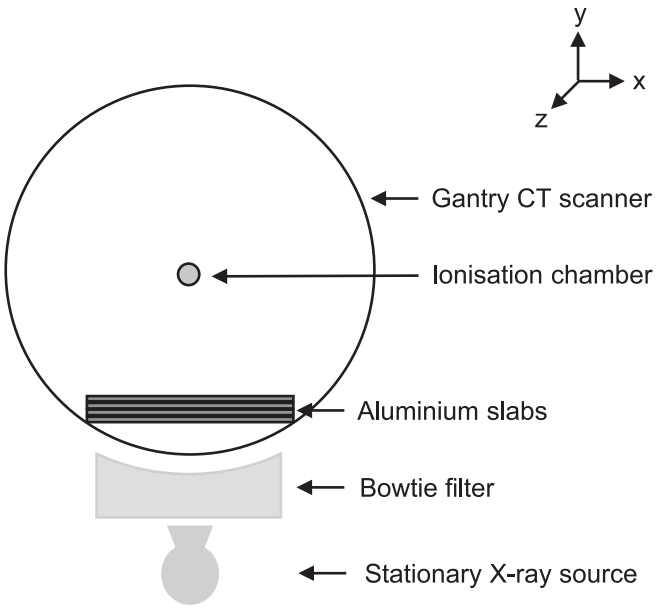

Fig. 4. Set-up of half-value layer measurement (based on Turner et al. [12]). The X-ray tube is kept stationary at the 6o'clock position and a calibrated ionisation chamber is placed at the isocenter of the CT. Aluminium slabs are stepwise added to the beam path, by placing them on the gantry, until the measured air kerma is less than half the initial air kerma measured without extra aluminium slabs in the beam path. All CT exposures are performed at a fixed tube current–time product.

an estimation of patient-specific organ doses D_T which were determined as follows:

$$D_T = \sum_{i=1}^{N} \left(f_{i,T} \bullet M_{i,T} \right) \; with \; f_{i,T} = \frac{A_{i,T}}{\sum_{i=1}^{N} A_{i,T}}$$

where $M_{i,T}$ is the mean dose within the contour at slice i of organ T, N the total number of slices that contain contours of organ T and $f_{i,T}$ the fractional area of each organ contour (with $A_{i,T}$ the area within the contour at slice i of organ T). To enable unsupervised organ dose calculation, an algorithm was implemented in Fiji/ImageJ. An overview of the complete workflow is given in Fig. 7.

2.5. Comparison of organ dose estimations

For each patient and each Monte Carlo simulation, using a different combination of X-ray spectrum and bowtie filter model, organ doses were calculated as described before. Next, the mean organ doses and their corresponding standard deviations were determined for the study population. For each organ, percentage dose differences were obtained by comparing the doses to those obtained using the quantitative model (s) provided by the manufacturer, which are assumed to be the ground truth. From these deviations the maximum value over all organs was determined for each studied situation. This was done to study the influence of both the used X-ray spectrum and bowtie filter model separately and their combinations.

3. Results

The mean CT organ doses and corresponding standard deviations of the breast, heart, liver, lungs, kidneys, ribs, thyroid, oesophagus and spine are shown in Fig. 8. As expected, deviations in organ doses were observed when a different combination of X-ray spectrum and bowtie filter model was used in the Monte Carlo simulation. For all organs, the estimated organ doses were the smallest when the X-ray spectrum provided by the manufacturer was applied while they were the largest when

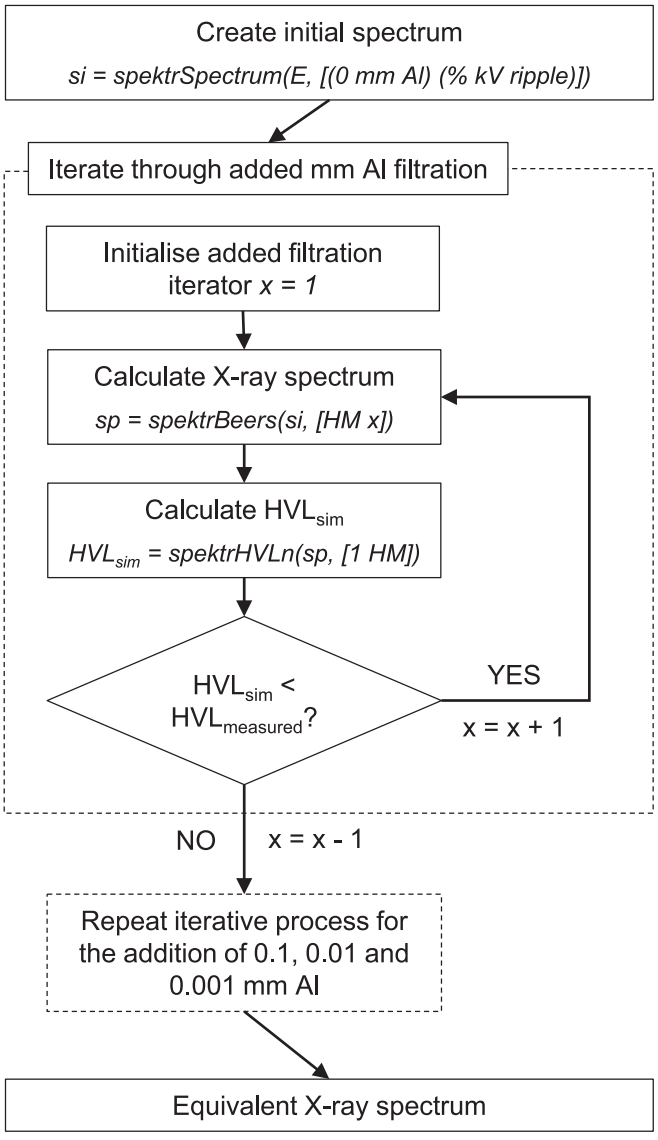

Fig. 5. Flowchart of the iterative process for the generation of equivalent X-ray spectra implemented in MATLAB: using the 'spektrSpectrum' function a soft spectrum *si* is created for an energy E of 120 kV without extra aluminium (Al) filtration and with a percentage voltage ripple of 0 % or 25 %. Secondly, 1 mm of aluminium filtration is added and by using the 'spektrBeers' function a new energy spectrum *sp* is created of which the first half-value layer HVL_{sim} is determined with the 'spektrHVLn' function. The simulated HVL value is then compared with the measured HVL value resulting from the ionisation chamber measurements. As long as the simulated HVL is lower, 1 mm extra aluminium filtration is added and a new energy spectrum *sp* and corresponding HVL_{sim} is calculated. When the simulated HVL is larger, 1 mm of aluminium is removed and the iterative process is repeated subsequently for the addition of 0.1 mm, 0.01 mm and 0.001 mm aluminium. Finally, an equivalent spectrum is created with a HVL that differs minimally from the measured HVL (E – energy (e.g. 120 kV), Al – aluminium, HM – hardening material (e.g. aluminium), HVL_{sim} – simulated half-value layer, $HVL_{measured}$ – measured half-value layer).

the spectrum generated with SpekCalc was used. Applying the manufacturer's bowtie filter model seemed to result in lower doses for most organs.

3.1. Influence of bowtie filter model

For each organ, dose differences were calculated when using the bowtie filter model based on dose measurements instead of the model

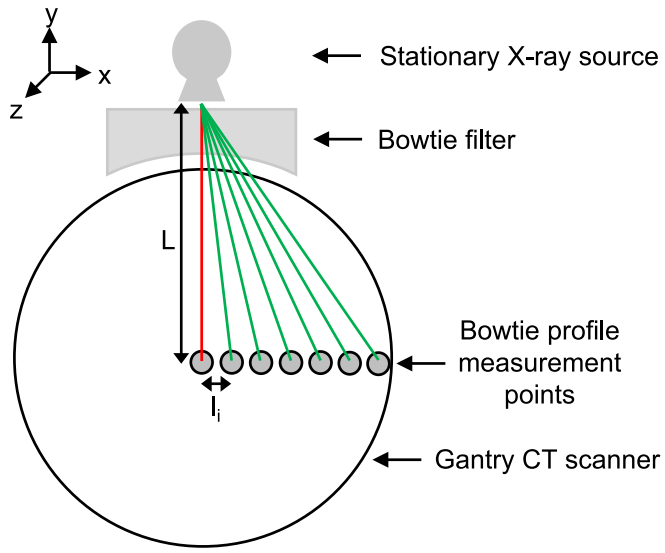

Fig. 6. Set-up of CT bowtie profile dose measurements, with L the focus to isocenter distance and l_i the distance between the measurement points (based on [12]). The X-ray tube is kept stationary at the 12 o'clock position. Dose measurements are performed using a calibrated ionisation chamber that is incrementally moved from the isocenter in +x and −x direction.

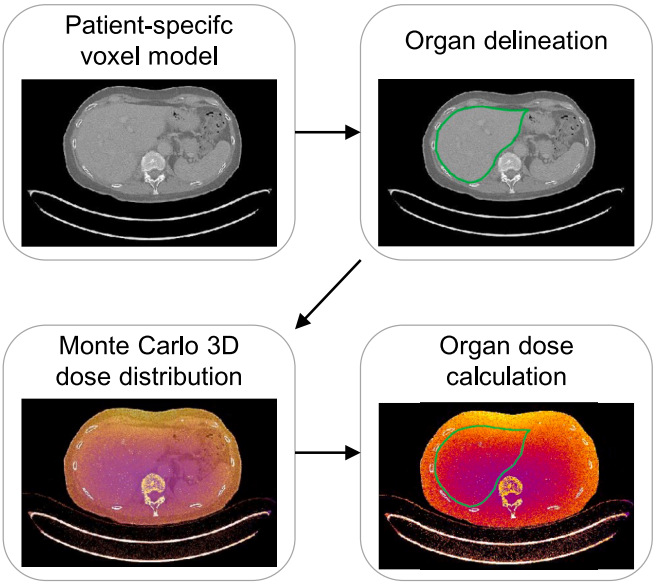

Fig. 7. Overview of the workflow – Whole-body CT images were used to create patient-specific 3D voxel models. Individual organs were delineated on the original CT images. The organ segmentations were used to calculate mean organ doses on the output images of the Monte Carlo simulations.

provided by the manufacturer, which is assumed to be the most accurate model. Fig. 9 shows the maximum percentage organ dose difference over all organs for each X-ray spectrum model. Maximum dose differences ranging from around 0.90% to 0.94% were observed.

3.2. Influence of X-ray spectrum model

Fig. 10 presents the maximum percentage difference in calculated CT organ dose between Monte Carlo simulations performed with and without the X-ray spectrum model based on the quantitative data from the manufacturer. Irrespective from the used bowtie filter model, organ dose differences up to 6% were observed. For Monte Carlo simulations performed with the equivalent X-ray spectrum with a 0% voltage ripple a maximum difference of 2.4% was found.

3.3. Influence of X-ray spectrum and bowtie filter model

Estimated CT organ doses were within 6% from those resulting from Monte Carlo simulations with the CT characterisation models provided by the manufacturer (Fig. 11). Disregarding all scenarios applying quantitative manufacturer's data, organ dose differences are within 5%. Dose differences smaller than 3% were found when the equivalent energy spectrum applying a 0% voltage ripple is used.

4. Discussion

Nowadays, Monte Carlo frameworks are the gold standard to perform patient-specific CT dosimetry. Besides allowing the implementation of anatomical 3D models, it also allows an accurate description of the CT scanner. Technical reference manuals already report specifications regarding the X-ray tube such as the anode angle and material. The inherent tube filtration, on the other hand, is often specified in equivalent aluminium thickness at a certain tube voltage. Similar conclusions can be made for the bowtie filter. If reported at all, the available bowtie filters are described in terms of quality equivalent filtration. However, information about the exact shape of the bowtie filter, or the varying filter thickness with increasing fan angle, is mostly missing. Specific details about the inherent filtration and bowtie filters, including the used material(s) and respective thickness(es), are the manufacturer's secret. Based on non-disclosure agreements, it is sometimes possible to obtain the necessary data to quantitatively model the X-ray spectrum and bowtie filter for a certain CT scanner from a specific manufacturer. Nevertheless, there are many CT scanners and gaining manufacturer's data is not always successful. Fortunately, methods exist to model X-ray spectra and bowtie filters based on little or no proprietary data.

As for Monte Carlo simulation tools, newly developed methodologies to characterise the X-ray spectrum and bowtie filter of a CT scanner are evaluated by comparing the accuracy of multiple CTDI simulations with

Table 3
Overview of the ten X-ray spectra and bowtie filter model combinations (scenarios).

X-ray spectrum and bowtie filter combination	120 kV X-ray spectrum model	Bowtie filter model
Sc 1a	Manufacturer	Manufacturer
Sc 1b	Manufacturer	Dose measurements
Sc 2a	Equivalent – 0% kV ripple	Manufacturer
Sc 2b	Equivalent – 0% kV ripple	Dose measurements
Sc 3a	Equivalent – 25% kV ripple	Manufacturer
Sc 3b	Equivalent – 25% kV ripple	Dose measurements
Sc 4a	ImpactMC generator	Manufacturer
Sc 4b	ImpactMC generator	Dose measurements
Sc 5a	SpekCalc	Manufacturer
Sc 5b	SpekCalc	Dose measurements

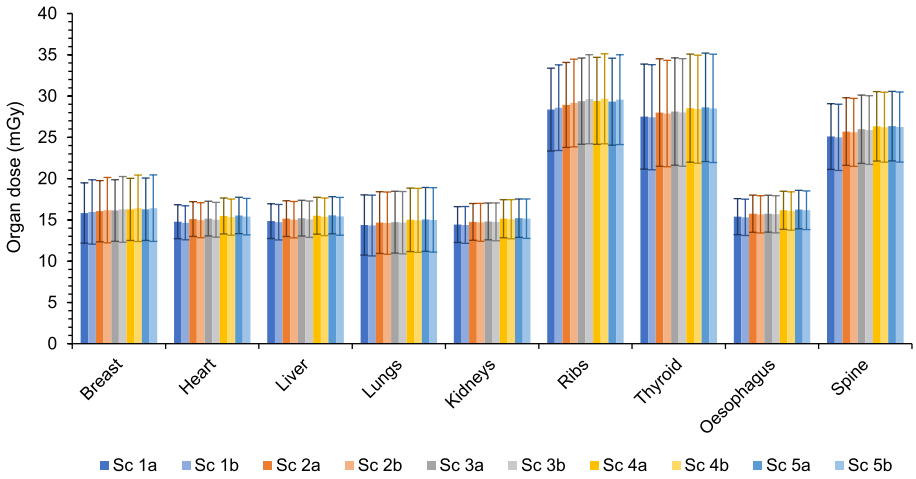

Fig. 8. Estimated mean organ doses of a diagnostic whole-body CT scan for each X-ray spectrum and bowtie filter model combination (spectrum: 1 –manufacturer, 2 – equivalent with 0% voltage ripple, 3 – equivalent with 25% voltage ripple, 4 – ImpactMC integrated generator, 5 – SpekCalc; bowtie filter: a – manufacturer, b – dose measurements).

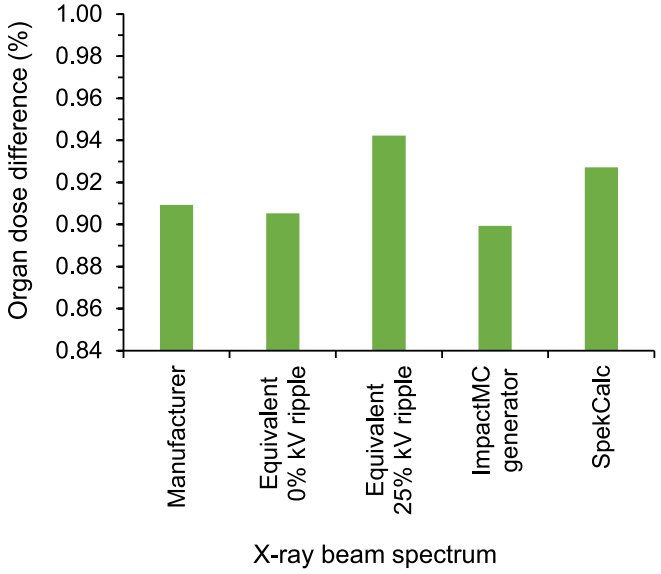

Fig. 9. Maximum percentage difference in calculated mean CT organ dose between the two bowtie filter models, for each X-ray spectrum model. Note that the assumption was made that the bowtie filter model provided by the manufacturer is the most accurate model.

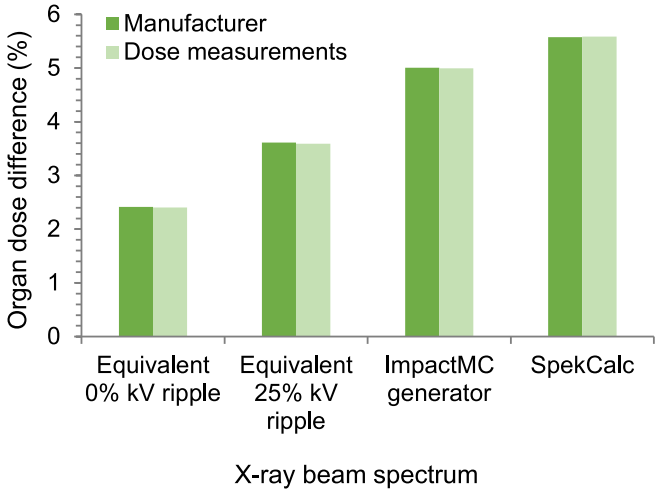

Fig. 10. Maximum percentage difference in calculated mean CT organ dose for the different X-ray spectrum models compared to the X-ray spectrum model provided by the manufacturer. Note that the assumption was made that the X-ray spectrum from the manufacturer is the most accurate model. Results are given for simulations performed with the bowtie filter model based on data from the manufacturer and dose measurements, respectively.

measured CTDI values. Depending on the specific study at hand, this is done for either or both standard IEC CT dosimetry phantoms [32]. Turner et al. [12], Kramer et al. [15] and Belinato et al. [33] reported an accuracy of approximately 95% while a deviation of even less than 4% was observed by Adrien et al. [34]. Nonetheless, the number of studies looking at the difference in simulated CT dose between Monte Carlo simulations performed using their own X-ray spectrum and bowtie filter models and those obtained from the manufacturer is limited. Using the IEC CT dosimetry phantoms, Turner et al. [12] found a difference of approximately 12% between the simulated CTDI values. Kramer et al. [15], on the other hand, showed a maximum deviation of about 6% between CTDI values simulated using their own developed bowtie filter model and the proprietary data made available by the manufacturer.

In this study, the accuracy of *patient-specific* organ doses obtained through Monte Carlo simulations applying different CT characterisation models was studied. Therefore, whole-body CT images of twenty adult patients were used as anatomy-specific voxel models. For each patient model, organ doses of a whole-body CT scan were calculated for each combination of five X-ray spectrum models and two bowtie filter models, including those based on quantitative manufacturer's data. The observed standard deviations are related to the wide range of BMI in the study population and the use of automatic tube current modulation.

For all organs, as expected, deviations in simulated CT organ doses are observed when the X-ray spectrum and bowtie filter were modelled in a different way. However, looking at the order of magnitude of the organ doses the impact is rather small. Modelling the bowtie filter based on dose measurements instead of using the one provided by the manufacturer leads to dose differences that are within 1%, irrespective of the applied X-ray spectrum model. This model is thus a very good alternative when no manufacturer's data about the bowtie filter is available. Considering only a variation in used X-ray spectrum determination method, CT organ doses within 6% from those resulting from simulations with the manufacturer spectrum are found. Even smaller deviations, smaller than 4%, are observed when the spectrum is modelled based on the methodology described by Turner et al. [12]. Similar

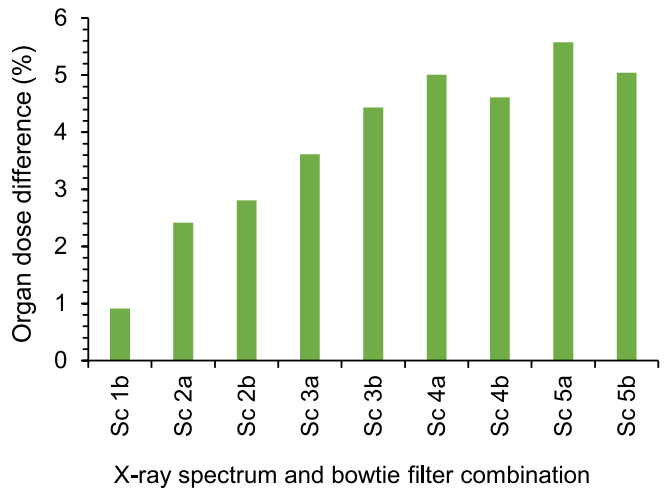

Fig. 11. Maximum percentage difference in calculated mean CT organ dose for the different X-ray spectrum and bowtie filter combinations (Sc 1b – Sc 5b) compared to scenario 1a (Sc 1a) that combines the X-ray spectrum and bowtie filter model provided by the manufacturer.

results are seen for both bowtie filter models. In the end, it is important to look at the combined effect of the applied bowtie filter and X-ray spectrum model. For all possible scenarios, organ doses are within 6% from the most accurate simulations using the models based on the data from the manufacturer. Disregarding all situations that make use of the quantitative data provided by the manufacturer, the best results are obtained by determining equivalent X-ray spectra with a voltage ripple of 0%. Organ dose differences are then within 3%. Half-value layer and dose measurements are thus good alternative methods to obtain equivalent X-ray spectra and bowtie filter profiles, respectively. Moreover, these measurements can be performed without special equipment and without the need to go into service mode.

Similar to Fig. 9 and Fig. 10, Fig. 11 presents the maximum percentage difference in calculated mean CT organ doses between different X-ray spectra and bowtie filter model combinations and the one combining the models provided by the manufacturer. Looking in more detail to the organ dose percentage differences for the scenarios that do not make use of any quantitative manufacturer's data, the following ranges are observed: 1.20% to 2.81%, 1.58% to 4.43%, 3.26% to 4.61% and 3.62% to 5.04% for scenarios 2b, 3b, 4b and 5b, respectively. The lowest values are found for the liver, heart and thyroid and they are within 0.5% of each other for each scenario. Also for the lungs a small deviation from the observed minimal percentage difference ($\leq$ 0.7%) is seen. For scenario 2b, 3b and 4b the largest percentage dose differences are related to the ribs, while for scenario 5b the largest difference is observed for the oesophagus. In general, these differences are quite small especially when taking into account the order of magnitude of the organ doses.

To our knowledge only Kramer et al. [15] eventually compared CT organ doses obtained through Monte Carlo simulation using their and the manufacturer's characterisation models for both the X-ray spectrum and bowtie filter. Organ dose differences within 8% and 6% were found for, respectively, simulations of a CT abdomen and CT thorax on a Philips Brilliance 64 CT scanner. Looking at the same organs as segmented in our study, their observed minimal organ dose differences were around 2.2% for both CT scans. These results are quite similar to those obtained in our research. However, the results of Kramer et al. [15] are calculated in the anthropomorphic MASH and FASH phantom for, respectively, a CT thorax and a CT abdomen scan [35].

One of the limitations of this study is that the results are based on one CT scanner from one manufacturer. Despite all attempts made, no quantitative spectral and bowtie filter profile data was obtained for a CT scanner from another manufacturer. Although obtaining the necessary proprietary data, even with a non-disclosure agreement, can take several weeks to months it can thus also be completely unsuccessful. Furthermore, the influence of the X-ray spectrum model on the accuracy of CT organ doses from Monte Carlo simulations was studied for one tube voltage, namely 120 kV which is the standard in diagnostic whole-body CT protocols in nuclear medicine applications. However, to obtain the X-ray spectrum model for other CT tube voltages the same methodologies can be used and similar results in accuracy are expected.

In order to implement patient-specific Monte Carlo dose simulations within the clinic, some requirements need to be fulfilled. First, the CT scanner needs to be characterised. As described before, the focus to isocenter distance and fan angle can be found in the technical reference manual or calculated from specific DICOM tags in the DICOM header of the CT images. Modelling the X-ray spectrum and bowtie filter must be done only once at acceptance of your device or, if preferred, whenever an X-ray tube or a bowtie filter is replaced. In a few hours it is possible to perform all necessary measurements to model the X-ray spectrum for each tube voltage and every available bowtie filter. At the same time, the air kerma free-in-air can be measured for each combination of tube voltage, collimation and bowtie filter, which is needed to calibrate the Monte Carlo software. Secondly, to perform patient-specific MC simulations of a CT scan, the CT scan parameters need to be given. The rotation time, pitch and applied beam collimation can be extracted from the examination protocols on the CT scanner. However, they can also easily be extracted from the DICOM header of the images together with the tube current values of each reconstructed image to integrate the tube current modulation. The time needed to run one Monte Carlo simulation depends on several factors. First of all, it depends on whether the computer on which the simulations run has a GPU or not. As can be expected, simulations run faster when a GPU is available instead of only a CPU. Also the generation of GPU plays a role. Next, the simulation time increases linearly with the number of simulated photons. Although the relative error in estimated organ dose decreases with the number of simulated photons, it is important to find a balance between the number of simulated photons and a realistic simulation time as the decrease in relative error eventually reaches a platform. Besides, the simulated scan length plays a role. The shorter the scan length, the faster the Monte Carlo simulation is done. Finally, organ segmentation may be very time consuming. However, the development of automatic segmentation tools, such as TotalSegmentator [36], and advances in deep learning create a lot of opportunities to speed up this process.

5. Conclusions

When manufacturer's data are not available, half-value layer and dose measurements, which can be performed without special equipment, provide sufficient input to obtain equivalent X-ray spectra and bowtie filter profiles, respectively. Monte Carlo simulations then result in estimated CT organ doses that deviate less than 3% from the most accurate simulations.

6. Author agreement

This article was setup in the framework of the MEDIRAD and SINFONIA projects. Data collection, Monte Carlo simulations and analysis of the results were performed by GV. Monte Carlo simulations and segmentations were partially performed by LD. The first draft was written by GV and all authors commented on previous versions of the manuscript. All authors read and approved the final manuscript.

Ethical Approval

The retrospective use of the CT images was approved by the medical ethics committee of Ghent University Hospital, Belgium (No. BC-06610 E01).

Funding

This study has received funding from the Euratom research and training programme 2014–2018 under grant agreement No. 755,523 and the Euratom research and innovation programme 2019–2020 under grant agreement No. 945196.

Declaration of competing interest

The authors declare that they have no known competing financial interests or personal relationships that could have appeared to influence the work reported in this paper.

Acknowledgements

The authors thank the Belgian team of Siemens Healthineers, Germany, for their efforts to provide quantitative spectral and bowtie filter data from the Siemens Biograph mCT Flow PET/CT.

References

[1] Alsafi KG. Radiation Protection in X-Ray Computed Tomography: Literature Review. International Journal of Radialogy and Imaging. Technology 2016;2.
[2] Franck C, Vandevoorde C, Goethals I, Smeets P, Achten E, Verstraete K, et al. The role of Size-Specific Dose Estimate (SSDE) in patient-specific organ dose and cancer risk estimation in paediatric chest and abdominopelvic CT examinations. Eur Radiol 2016;26:2646–55. https://doi.org/10.1007/s00330-015-4091-7.
[3] Aapm. Size-Specific Dose Estimates (SSDE) in pediatric and adult body ct examinations (Task Group 204). American Association of Physicists in Medicine 2011.
[4] Aapm. Use of water equivalent diameter for calculating patient size and Size-Specific Dose Estimate (SSDE) in CT (Task Group 220). American Association of Physicists in Medicine 2014.
[5] Stamm G, Nagel HD. CT-Expo - a novel program for dose evaluation in CT. Rofo 2002;174:1570–6. https://doi.org/10.1055/s-2002-35937.
[6] Ban N, Takahashi F, Sato K, Endo A, Ono K, Hasegawa T, et al. Development of a web-based CT dose calculator: WAZA-ARI. Radiat Prot Dosimetry 2011;147:333–7. https://doi.org/10.1093/rpd/ncr333.
[7] Ding AP, Gao YM, Liu HK, Caracappa PF, Long DJ, Bolch WE, et al. VirtualDose: a software for reporting organ doses from CT for adult and pediatric patients. Phys Med Biol 2015;60:5601–25. https://doi.org/10.1088/0031-9155/60/14/5601.
[8] Lee C, Kim KP, Bolch WE, Moroz BE, Folio L. NCICT: a computational solution to estimate organ doses for pediatric and adult patients undergoing CT scans. J Radiol Prot 2015;35:891–909. https://doi.org/10.1088/0952-4746/35/4/891.
[9] Sato K, Noguchi H, Emoto Y, Koga S, Saito K. Japanese adult male voxel phantom constructed on the basis of CT images. Radiat Prot Dosim 2007;123:337–44. https://doi.org/10.1093/rpd/ncl101.
[10] Tucker DM, Barnes GT, Chakraborty DP. Semiempirical model for generating tungsten target x-ray spectra. Med Phys 1991;18:211–8. https://doi.org/10.1118/1.596709.
[11] Poludniowski G, Landry G, DeBlois F, Evans PM, Verhaegen F. SpekCalc: a program to calculate photon spectra from tungsten anode x-ray tubes. Phys Med Biol 2009;54:N433. https://doi.org/10.1088/0031-9155/54/19/N01.
[12] Turner AC, Zhang D, Kim HJ, DeMarco JJ, Cagnon CH, Angel E, et al. A method to generate equivalent energy spectra and filtration models based on measurement for multidetector CT Monte Carlo dosimetry simulations. Med Phys 2009;36:2154–64. https://doi.org/10.1118/1.3117683.
[13] Boone JM. Method for evaluating bow tie filter angle-dependent attenuation in CT: theory and simulation results. Med Phys 2010;37:40–8. https://doi.org/10.1118/1.3264616.
[14] McKenney SE, Nosratieh A, Gelskey D, Yang K, Huang SY, Chen L, et al. Experimental validation of a method characterizing bow tie filters in CT scanners using a real-time dose probe. Med Phys 2011;38:1406–15. https://doi.org/10.1118/1.3551990.
[15] Kramer R, Cassola VF, Andrade MEA, de Araújo MWC, Brenner DJ, Khoury HJ. Mathematical modelling of scanner-specific bowtie filters for Monte Carlo CT dosimetry. Phys Med Biol 2017;62:781–809. https://doi.org/10.1088/1361-6560/aa5343.
[16] Chen W, Kolditz D, Beister M, Bohle R, Kalender WA. Fast on-site Monte Carlo tool for dose calculations in CT applications. Med Phys 2012;39:2985–96. https://doi.org/10.1118/1.4711748.
[17] Deak P, van Straten M, Shrimpton PC, Zankl M, Kalender WA. Validation of a Monte Carlo tool for patient-specific dose simulations in multi-slice computed tomography. Eur Radiol 2008;18:759–72. https://doi.org/10.1007/s00330-007-0815-7.
[18] Schmidt B, Kalender WA. A fast voxel-based Monte Carlo method for scanner- and patient-specific dose calculations in computed tomography. Phys Medica 2002;18:43–53.
[19] Myronakis M, Perisinakis K, Tzedakis A, Gourtsoyianni S, Damilakis J. Evaluation of a patient-specific Monte Carlo software for CT dosimetry. Radiat Prot Dosim 2009;133:248–55. https://doi.org/10.1093/rpd/ncp051.
[20] Mulkens TH, Bellinck P, Baeyaert M, Ghysen D, Van Dijck X, Mussen E, et al. Use of an automatic exposure control mechanism for dose optimization in multi-detector row CT examinations: Clinical evaluation. Radiology 2005;237:213–23. https://doi.org/10.1148/radiol.2363041220.
[21] Rizzo S, Kalra M, Schmidt B, Dalal T, Suess C, Flohr T, et al. Comparison of angular and combined automatic tube current modulation techniques with constant tube current CT of the abdomen and pelvis. Am J Roentgenol 2006;186:673–9. https://doi.org/10.2214/Ajr.04.1513.
[22] Rego SL, Yu L, Bruesewitz MR, Vrieze TJ, Kofler JM, McCollough CH. CARE Dose4D CT automatic exposure control system. physics principles and practical hints. Mayo Foundation for Medical Education and Research; 2008.
[23] Soderberg M, Gunnarsson M. The effect of different adaptation strengths on image quality and radiation dose using Siemens Care Dose 4D. Radiat Prot Dosim 2010;139:173–9. https://doi.org/10.1093/rpd/ncq098.
[24] Papadakis AE, Perisinakis K, Damilakis J. Automatic exposure control in CT: the effect of patient size, anatomical region and prescribed modulation strength on tube current and image quality. Eur Radiol 2014;24:2520–31. https://doi.org/10.1007/s00330-014-3309-4.
[25] Soderberg M. Overview, Practicaltips and Potential Pitfalls of Using Automatic Exposure Control in Ct: Siemens Care Dose 4d. Radiat Prot Dosim 2016;169:84–91. https://doi.org/10.1093/rpd/ncv459.
[26] User Guide ImpactMC. CT Imaging GmbH; 2010-2016.
[27] Siewerdsen JH, Waese AM, Moseley DJ, Richard S, Jaffray DA. Spektr: a computational tool for x-ray spectral analysis and imaging system optimization. Med Phys 2004;31:3057–67. https://doi.org/10.1118/1.1758350.
[28] Yang K, Li XH, Xu XG, Liu B. Direct and fast measurement of CT beam filter profiles with simultaneous geometrical calibration. Med Phys 2017;44:57–70. https://doi.org/10.1002/mp.12024.
[29] Schindelin J, Arganda-Carreras I, Frise E, Kaynig V, Longair M, Pietzsch T, et al. Fiji: an open-source platform for biological-image analysis. Nat Methods 2012;9:676–82. https://doi.org/10.1038/nmeth.2019.
[30] Schneider CA, Rasband WS, Eliceiri KW. NIH Image to ImageJ: 25 years of image analysis. Nat Methods 2012;9:671–5. https://doi.org/10.1038/nmeth.2089.
[31] Fedorov A, Beichel R, Kalpathy-Cramer J, Finet J, Fillion-Robin JC, Pujol S, et al. 3D Slicer as an image computing platform for the Quantitative Imaging Network. Magn Reson Imaging 2012;30:1323–41. https://doi.org/10.1016/j.mri.2012.05.001.
[32] IEC. IEC 60601-2-44:2009+AMD1:2012+AMD2:2016 ed3.2 Medical electrical equipment - Part 2-44: Particular requirements for the basic safety and essential performance of X-ray equipment for computed tomography2016.
[33] Belinato W, Santos WS, Paschoal CMM, Souza DN. Monte Carlo simulations in multi-detector CT (MDCT) for two PET/CT scanner models using MASH and FASH adult phantoms. Nucl Instrum Meth A 2015;784:524–30. https://doi.org/10.1016/j.nima.2014.09.036.
[34] Adrien C, Le Loirec C, Dreuil S, Bordy JM. A new Monte Carlo tool for organ dose estimation in computed tomography. Radioprotection 2020;55:123–34. https://doi.org/10.1051/radiopro/2020006.
[35] Cassola VF, Kramer R, Brayner C, Khoury HJ. Posture-specific phantoms representing female and male adults in Monte Carlo-based simulations for radiological protection. Phys Med Biol 2010;55:4399–430. https://doi.org/10.1088/0031-9155/55/15/014.
[36] Wasserthal J, Breit HC, Meyer MT, Pradella M, Hinck D, Sauter AW, et al. TotalSegmentator: robust segmentation of 104 anatomic structures in CT images. Radiol-Artif Intell 2023;5. ARTN e23002410.1148/ryai.230024.